

Crystal chemistry of lunar merrillite and comparison to other meteoritic and planetary suites of whitlockite and merrillite

BRADLEY L. JOLLIFF,^{1,*} JOHN M. HUGHES,² JOHN J. FREEMAN,¹ AND RYAN A. ZEIGLER¹

¹Department of Earth and Planetary Sciences, Washington University, St. Louis, Missouri 63130, U.S.A.

²Office of the Provost, 348B Waterman Building, University of Vermont, Burlington, Vermont 05405, U.S.A.

ABSTRACT

Merrillite, also known as “whitlockite,” is one of the main phosphate minerals, along with apatite, that occur in lunar rocks, martian meteorites, and in many other groups of meteorites. Significant structural differences between terrestrial whitlockite and lunar (and meteoritic) varieties warrant the use of “merrillite” for the H-free extraterrestrial material, and the systematic enrichment of REE in lunar merrillite warrants the use of “RE-merrillite.” Laser Raman spectroscopy of extraterrestrial merrillite and terrestrial whitlockite confirms the absence of H in the former and presence of H in the latter. Lunar merrillite, ideally $(\text{Mg, Fe}^{2+}, \text{Mn}^{2+})_2[\text{Ca}_{18-x}(\text{Y, REE})_x](\text{Na}_{2-x})(\text{P, Si})_{14}\text{O}_{56}$, contains high concentrations of Y+REE, reaching just over 3 atoms per 56 O atoms, or up to ~18 wt% as $(\text{Y, RE})_2\text{O}_3$. In the absence of extensive Si \leftrightarrow P substitution, the “availability” of the Na site limits Y+REE substitution to ~2 atoms per 56 O atoms. Higher concentrations of Y+REE, with coupled substitution of Si for P to balance charge are possible, but rare in lunar material. Intrinsically low Na concentrations in lunar rocks, combined with the typical formation of merrillite in late-stage basaltic mesostasis or residual, intercumulus melt pockets, produce these high REE concentrations. Lunar merrillite typically contains 0.1–0.4 Na atoms per 56 O atoms. For comparison, martian merrillite contains significantly higher Na concentrations (up to 1.7 Na atoms per 56 O atoms) and much lower REE concentrations. Meteoritic merrillite has relatively low REE contents, but exists in both Ca-rich and Na-rich varieties. Concentrations of Fe and Mg in all varieties sum to near 2 atoms per 56 O atoms. Merrillite in lunar crustal lithologies typically has Mg \gg Fe; however, Fe-rich mare basalts contain up to 1.8 Fe²⁺ per 56 O. The structure of merrillite accommodates a variety of substitutions, and the compositional characteristics reflect conditions and processes specific to the parent planet.

Keywords: Merrillite, whitlockite, Moon, Mars, electron microprobe, ion microprobe, Raman spectroscopy, rare earth elements

INTRODUCTION

Merrillite, which has also been referred to in previous literature as “whitlockite,” is an important accessory mineral in lunar rocks and in meteorites. Studies of this accessory phase have provided insights into the petrogenesis of extraterrestrial rocks (e.g., in meteorites: Delaney et al. 1984; Reed and Smith 1985; Davis and Olsen 1991; and in lunar rocks: Fuchs 1971; Griffin et al. 1972; James et al. 1987; Lindstrom et al. 1985; Jolliff et al. 1993; Chambers et al. 1995, and many others). It is one of the two most common phosphates in extraterrestrial rocks, the other being apatite. Other phosphates including farringtonite $(\text{Mg, Fe})_3(\text{PO}_4)_2$ (Dowty et al. 1974), and monazite $(\text{Ce, La, Nd, Th})\text{PO}_4$ (Lovering et al. 1974; Jolliff 1993) have been reported in lunar rocks, but these are rare. A wide variety of phosphates have been found in meteorites (see Rubin 1997), and merrillite is found in most meteorite groups. Apatite and merrillite are the two principal phosphates found in martian meteorites (e.g., McSween 1994; McSween and Treiman 1998; Greenwood et al. 2003).

Early work on lunar samples suggested that “lunar whitlockite” is similar in structure to meteoritic merrillite (Gay et al. 1970; Fuchs

1971); however, the lunar material was generally too fine-grained to yield a definitive structural refinement. X-ray structural refinements of meteoritic material showed their structures to be similar, but not identical, to that of terrestrial whitlockite (Calvo and Gopal 1975; Prewitt and Rothbard 1975; Dowty 1977). Dowty, who refined the structure of *whitlockite* from the Angra Dos Reis meteorite, recommended the use of *merrillite* for the extraterrestrial variety on the basis that the lack of H led to a fundamental structural difference between the extraterrestrial and terrestrial varieties, and merrillite was revalidated by the Commission on New Minerals, Nomenclature and Classification of the International Mineralogical Association (IMA) at that time. In a companion paper in this issue, Hughes et al. (2006) present the first X-ray structural refinement of a lunar grain and we recommend, along the same lines of argument as Dowty, the use of *merrillite* for the lunar mineral because of significant and systematic structural and chemical compositional differences from terrestrial whitlockite. Hereafter, we refer to the extraterrestrial (and synthetic), H-free material as *merrillite*. In this paper, we discuss the crystal chemistry and compositional variations among different samples of lunar merrillite and compare them to merrillite found in martian rocks (meteorites) and some other meteorites.

Most lunar rocks contain at least a trace of apatite or merrillite, or both. In rocks that bear a “KREEP” signature, that is,

* E-mail: blj@levee.wustl.edu

a characteristic enrichment of incompatible minor and trace elements including K, REE, and P (as well as Ba, Rb, Cs, Zr, Hf, Nb, Ta, Th, and U), merrillite is almost always present and typically occurs along with apatite. In some cases, composite phosphate grains consist of an intergrowth of the two minerals (e.g., Jolliff et al. 1993, their Figs. 2b and 2e). Frondel (1975) and Smith and Steele (1976) summarized occurrences, forms, and chemical compositions of lunar phosphates. Our intent in the present paper is to explore the range of compositional variations and substitution mechanisms in lunar merrillite, and to highlight those aspects of chemical composition that set lunar merrillite apart from its martian and meteoritic counterparts, and from terrestrial whitlockite.

METHODS

The results reported in this paper were obtained by several microbeam methods. Major and minor elements, including the most abundant of the REE, were determined using the electron microprobe. Rare earth elements (REE) were determined for a subset of the merrillite samples using the ion microprobe (e.g., Lindstrom et al. 1985; Lundberg et al. 1988; Davis and Olsen 1991; and Jolliff et al. 1993). We have also analyzed merrillite with the laser Raman microprobe to compare its spectrum to that of terrestrial whitlockite and synthetic merrillite.

Electron microprobe

We analyzed merrillite using the JEOL733 electron microprobe located at Washington University in the Department of Earth and Planetary Sciences. We used an accelerating voltage of 15 kV and beam currents ranging from 20 to 40 nA for wavelength-dispersive, quantitative analyses. For analyses of the relatively light elements (Na, F, P, Si, Mg, Ca), we used a 20 nA beam current. For Y, REE, and Sr, we used either 30 or 40 nA. Several elements were analyzed in both routines, including P, Ca, and Fe. To avoid volatilization of F and Na, we used an electron beam broadened to 5–10 μm wherever possible.

For calibration, we used a combination of mineral, oxide, and glass standards. We used a natural apatite for P and Ca, enstatite for Mg and Si, fayalite for Fe, albite or sodalite for Na, rhodonite for Mn, kyanite for Al, a synthetic Sr feldspar for Sr, and fluorphlogopite for F. Although a fluorapatite can be used as the calibration standard for F, caution is needed to be sure the peak selected for F is indeed F and not the nearby strong third-order phosphorous peak (e.g., at ~ 201 on TAP compared to the relatively weak F peak at ~ 199 on TAP) (e.g., Shervais et al. 1985). Use of the fluorphlogopite as a calibration standard avoids the potential for erroneous peaking on the P line. We used rare-earth orthophosphates (Jarosewich and Boatner 1991) to calibrate the REE. We used natural apatite and merrillite samples and REE-doped glasses (Drake and Weill 1972) as calibration monitors for the phosphates.

Data reduction procedures incorporated X-ray matrix corrections according to a modified (Armstrong 1988) CIT-ZAF routine (through Advanced Microbeam Probe for Windows) software (e.g., Donovan and Tingle 1996). For partial analyses (e.g., light elements vs. heavy elements), values must be corrected for matrix effects using the entire suite of elements, including those that were analyzed and those (REE) whose concentrations were estimated by interpolation/extrapolation.

Ion microprobe

The concentrations of REE and other trace elements were measured in carbon-coated thin sections using a modified Cameca 3-f ion microprobe (or secondary ion mass spectrometer, SIMS) at Washington University according to methods given by Zinner and Crozaz (1986). The specific procedures used to measure the REE can be found in Jolliff et al. (1993). Calcium contents determined by electron microprobe were used to normalize the ion signals. Systematic errors between SIMS and electron microprobe analyses were discussed in Jolliff et al. (1993). Because Ce and Y can be measured very accurately with the electron microprobe, Jolliff et al. (1993) adopted an approach of using Ce from the electron microprobe analyses to fix Ce determined by SIMS. The

abundances of the other REE relative to Ce from the SIMS data were then used to determine concentrations. This method also helps to mitigate against the effects of compositional heterogeneity and ensure that the REE concentrations are those that correspond to the rest of the elements measured by the electron microprobe. From the coupled EMP and SIMS analyses, we find that in the chondrite-normalized REE pattern, Y plots very close to Ho and Er (see also the Springwater Pallasite merrillite, Olsen and Davis 1991) (Fig. 1). This is not surprising because the ionic radii of Ho^{3+} and Er^{3+} are very similar to that of Y^{3+} .

Laser Raman spectroscopy

Raman spectra were obtained initially with an ISA U-1000 laser Raman microprobe at Washington University and were first reported in Jolliff et al. (1996). More recently, we have re-measured the Raman spectra of the terrestrial whitlockite and lunar merrillite using a Kaiser Raman Holoprobe, again at Washington University, confirming the spectral features identified with the U-1000. The laser Raman microprobe system employs an optical microscope coupled to a Raman spectrometer fitted with a CCD array detector. The whitlockite and merrillite samples were irradiated with ~ 20 mW of 532 nm Nd-YAG, frequency-doubled, laser radiation through the microscope objective, and the back-scattered Raman light was collected through the same microscope objective (20 to 80 \times). The spectral information was collected in the 0 to 2000 cm^{-1} region (U-1000) or 0 to 4000 cm^{-1} region (Kaiser Holoprobe) with software provided by the instrument manufacturers.

Raman vibrational spectroscopy, like its infrared counterpart, uses chemical functional-group frequency analysis to identify the principal molecular components of the mineral. The Raman vibrational spectra are also sensitive to the crystallographic site symmetry of the mineral, which permits distinction among crystallographically similar structures or between different polymorphs of the same chemical compound. The laser Raman microprobe can be used to obtain spectral information, non-destructively, in-situ, from sample grains as small as 3 μm , and such an analysis can be made on loose, unprepared rock fragments.

CRYSTAL STRUCTURE

We present here a brief summary of the crystal structure of merrillite as a framework for the discussion of chemical compositions. More detailed discussions can be found in Hughes et al. (2006, this issue) and references therein, especially Calvo

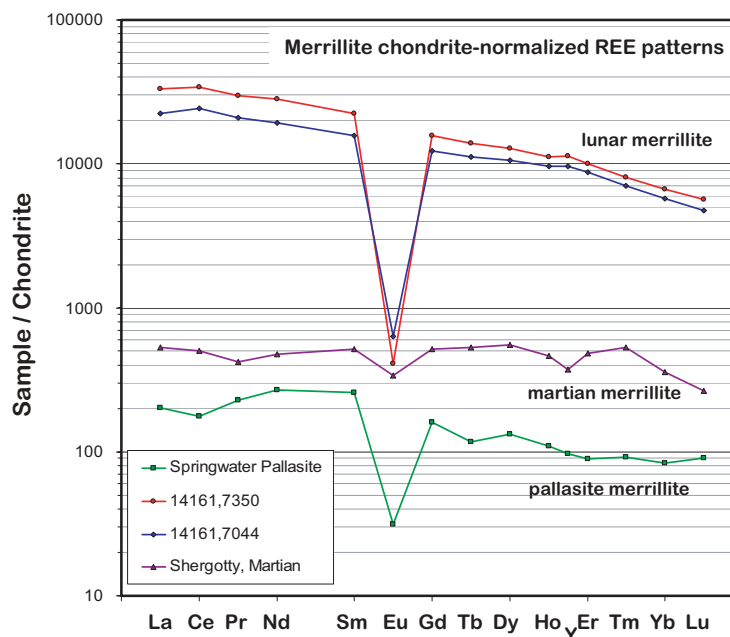


FIGURE 1. Chondrite-normalized REE patterns of merrillite grains that have been analyzed with the ion microprobe. Note the relatively smooth patterns of the lunar merrillite and the close correspondence of chondrite-normalized Y to Ho and Er. Lunar examples from Jolliff et al. 1993; martian example from Lundberg et al. 1988, and pallasite example from Olsen and Davis 1991. Values for chondrite normalization are from Anders and Grevesse (1989) multiplied by a factor of 1.36.

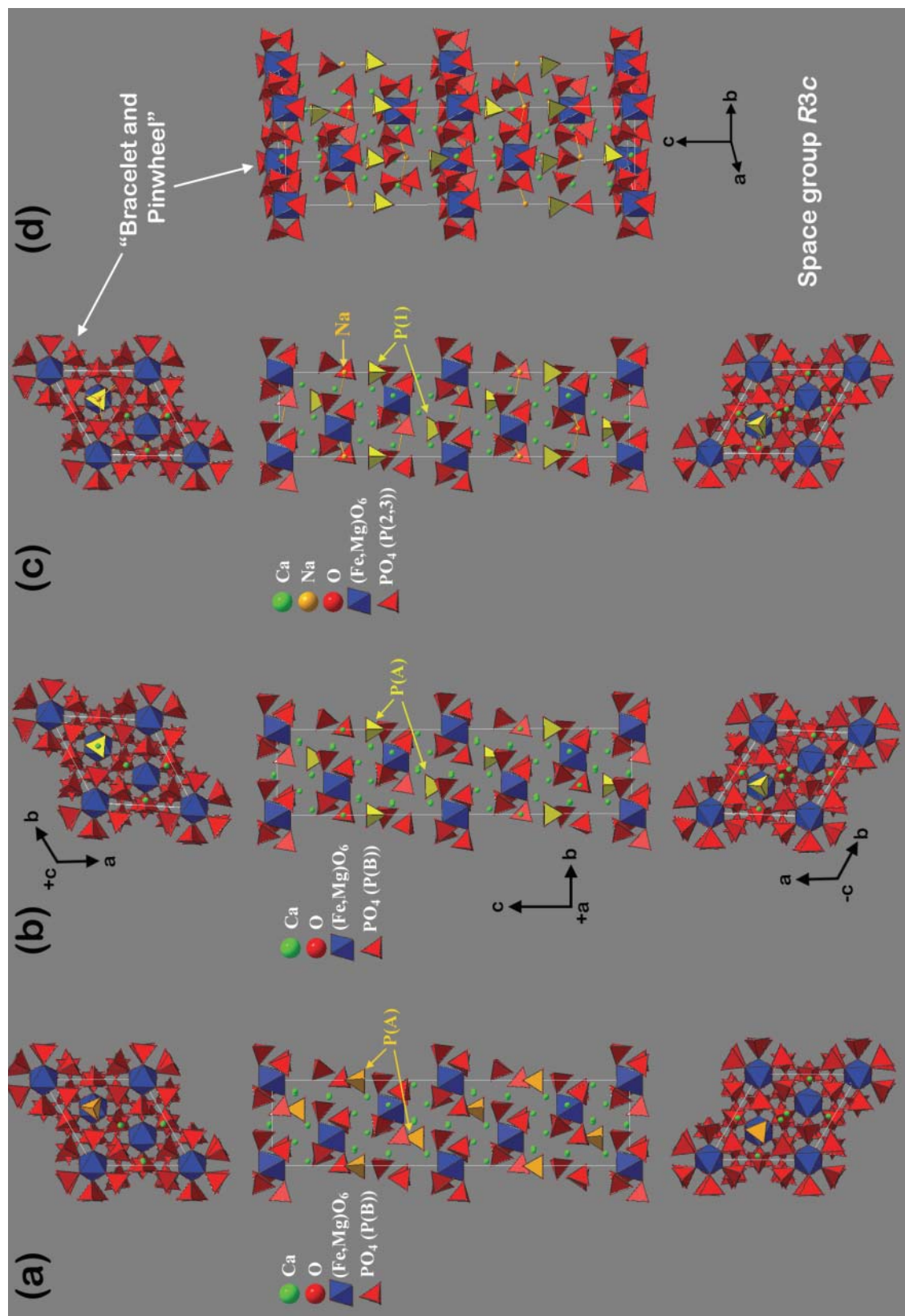


FIGURE 2. Comparison of structures of (a) terrestrial whitlockite (Palemo; Calvo and Gopal 1975), (b) meteoritic Ca-merrillite (Angra dos Reis Achondrite; Dowty 1977), and lunar RE-merrillite (14161, 7373; Hughes et al. 2006). Projections are along *c* (+*c*, -*c*) and along *a* (+*a*). Note the “bracelet and pinwheel” structural arrangement of phosphate tetrahedra arrayed around Mg,Fe octahedra in the projections along the *c* axis, discussed in Hughes et al. (2006). In **a**, P(A) tetrahedra are colored gold. In **b**, P(A) tetrahedra are colored yellow and are inverted relative to **a**. In **c**, P(1) phosphate tetrahedra on the triad axis are colored yellow; Na and shortest Na-O bonds are colored gold. In **d**, the structure is rotated about the *c* axis relative to **c**. Drawings were made with the program Diamond 2.1e by Klaus Brandenburg.

and Gopal (1975), Prewitt and Rothbard (1975), and Dowty (1977).

Using powder X-ray diffraction (XRD), Gopal and Calvo (1972) showed that the structure of whitlockite differs from that of synthetic, anhydrous β - $\text{Ca}_3(\text{PO}_4)_2$ by the inversion of one of the phosphate tetrahedra (see below). It was postulated that the apical oxygen atom of this tetrahedron was an hydroxyl ion. Gopal et al. (1974) reported that whitlockite loses its H on heating to temperatures above 700 °C.

In the whitlockite and merrillite structures, there are three symmetrically distinct phosphate tetrahedra. For every 56 O atoms, there are two P1 (PA'), six P2 (PB1) and six P3 (PB2) groups [using the nomenclature of Hughes et al. 2006 (with that of Calvo and Gopal 1975, in parentheses)]. Subsequent to the earlier work of Gopal and Calvo (1972), XRD studies of terrestrial whitlockite (Calvo and Gopal 1975), meteoritic merrillite (Prewitt and Rothbard 1975; Dowty 1977), and lunar merrillite (Hughes et al. 2006) have shown results that are consistent with inversion of the P1 tetrahedra, which essentially opens up an additional octahedral site in the H-free β - $\text{Ca}_3(\text{PO}_4)_2$ structure. We refer to these as "Na sites" and they correspond to the "CaIIA" sites of Calvo and Gopal (1975) and Dowty (1977).

The main Ca sites in merrillite, referred to as Ca1, Ca2, and Ca3 (or "CaB sites" of previous studies) are 8-coordinated, and 18 such general sites occur per 56 O atoms. Two special, smaller octahedral sites are designated "Mg sites" and preferentially host Mg, Fe, and Mn. The special "Na sites" form irregular octahedra. In merrillite, stoichiometry restricts these sites to 50% occupancy if by divalent Ca [relative to $\text{Ca}_3(\text{PO}_4)_2$, i.e., $\text{Ca}_{21}(\text{PO}_4)_{14}$]. In terrestrial whitlockite, the H ions occur in the same location as the Na sites (or CaIIA sites) in merrillite.

Two Na atoms can be accommodated per 56 O atoms (Hughes et al. 2006) or the site can be vacant as a charge-balancing mechanism for trivalent-ion substitution on the general Ca sites, as for example, the trivalent REE (e.g., Dowty 1977). In lunar merrillite, the substitution of trivalent REE for divalent Ca coupled with a vacancy on the Na sites appears to be an energetically favorable mechanism as well as a means of charge balance. This substitution was discussed at length in Jolliff et al. (1993) and will be discussed below following presentation of compositional data. The site occupancy variations are summarized in Table 1 where we refer to the end-members as Ca-merrillite, Na-merrillite, and RE-merrillite.

The replacement of P^{5+} by Si^{4+} is another potential mechanism for coupled substitution of REE^{3+} for Ca^{2+} . This mechanism is common in terrestrial apatite and has been found to be a viable mechanism in synthetic merrillite (McKay et al. 1987; Colson et al. 1992). This coupled substitution is also listed in Table 1. The structures of several variations, including terrestrial whitlockite, meteoritic merrillite, and lunar merrillite, are illustrated

in Figure 2.

On the basis of the structural differences associated with essential H in terrestrial whitlockite and lack of H in the extraterrestrial material, it was recommended (Calvo and Gopal 1975; Dowty 1977) that H-free whitlockite be considered a different mineral from terrestrial whitlockite and formally named merrillite. In this paper and in Hughes et al. (2006, this issue), we provide structural and compositional evidence in support of this recommendation.

DATA SET AND UNCERTAINTIES ASSOCIATED WITH COMPOSITIONAL MEASUREMENTS

In this paper, we list a selected set of merrillite samples (Table 2) and their compositions (Table 3). Most of the samples listed are lunar materials, and these represent a subset of many compositions that appear in the literature. In this work, we focus on coupled substitutions that involve Si, Na, Y, and the REE, thus we only consider published analyses that include these elements or our own analyses of samples (with previously published compositions) where we have determined the missing elements or have done a completely new analysis (most cases). We include several analyses of martian merrillite to establish the general compositional features that appear to characterize them. We also include a meteoritic merrillite from a pallasite (Davis and Olsen 1991) for comparison. The criteria that we used to select compositions for this paper were as follows: P+Si must sum to near 14 cations per 56 O atoms and the analysis must include Fe, Mg, Si, and Na. All lunar analyses must include Y and Ce at a minimum for the REE. Most of the compositions listed in Table 3 have tetrahedral cation sums (P+Si) between 13.85 and 14.1, and the average is 13.98.

Sources of uncertainty

Several sources of uncertainty stemming from analytical issues pertain to our ability to calculate stoichiometry for merrillite. First is the analysis of the two major elements, Ca and P. For analyses of calcium and phosphate standards, we typically obtain a standard deviation of 1–1.3% relative on CaO and P_2O_5 . For multiple analyses of merrillite in samples such as the 14161,7xxx set (see below), we obtain an average standard deviation within this same range. Thus, uncertainties associated with the measurement of P correspond to a potential uncertainty of ± 0.06 tetrahedral cations per 56 O atoms, and that associated with Ca is ± 0.05 tetrahedral cations per 56 O atoms.

Another important potential source of error relates to the analysis of the REEs. Errors associated with uncertainties in the measurement of the REEs where we have ion-microprobe data (multiple to many spots per rock sample) average about ± 5 –6% relative for the sum $(\text{Y}+\text{REE})_2\text{O}_3$. This uncertainty translates to about ± 0.03 tetrahedral cations per 56 O atoms. Errors associated with estimating REE concentrations when only a few elements are analyzed with the electron microprobe have a similar effect as long as either Ce or Y are within 10% of the true value. Thus, we conclude that uncertainties associated with analysis of Ca and P are likely to be of the same order of magnitude as (or greater than) uncertainties introduced by the measurement and estimation of the full suite of REEs. If the more abundant REEs (including Y, La, Ce, Nd, Sm, Gd, Dy, and Er) can be measured

TABLE 1. Merrillite end-members and site occupancies

Site	Ca(B)	"Mg site"	Na site [Ca(IIA)]	P site
coordination	8-coord	octahedral	irreg. oct.	tetrahedral
multiplicity (per 56 O atoms)	18	2	2	14
Ca-Merrillite	Ca_{18}	$(\text{Mg,Fe,Mn})_2$	$\text{Ca}_1\Box_1$	P_{14}
Na-Merrillite	Ca_{18}	$(\text{Mg,Fe,Mn})_2$	Na_2	P_{14}
RE-Merrillite	$\text{REE}_2\text{Ca}_{16}$	$(\text{Mg,Fe,Mn})_2$	\Box_2	P_{14}
Si-REE exchange	$\text{REE}_x\text{Ca}_{18-x}$	$(\text{Mg,Fe,Mn})_2$	\Box_2	$\text{Si}_x\text{P}_{14-x}$

TABLE 2. Merrillite-bearing samples

Samples	Lithology	Notes	Analysis	Key reference
lunar				
14161,7350	magnesian anorthosite	composite grain of apatite and merrillite	EMP, SIMS	Jolliff et al. 1993
14161,7373	monzogabbro	merrillite-rich, apatite minor;	EMP, SIMS	Jolliff et al. 1993
14161,7044	shocked gabbro	merrillite relatively coarse apatite and merrillite occur in intergranular spaces	EMP, SIMS	Jolliff et al. 1993
14161,7264	monzogabbro breccia	merrillite and apatite occur in monzogabbro clast	EMP, SIMS	Jolliff et al. 1993
14161,7233	impact-melt rock	incompatible elements 3× high-K KREEP; merrillite and apatite	EMP, SIMS	Jolliff et al. 1993
14161,7069	quartz monzodiorite (monzogabbro)	abundant fine-grained merrillite and apatite	EMP, SIMS	Jolliff et al. 1993
10085	shocked Ti-rich basaltic rock	Y+LREE through Nd measured, others extrapolated	EMP	Albee and Chodos 1970
12036,9	coarse-grained olivine basalt	several of the more abundant REE measured, others interpolated (see Table 3)	EMP	Keil et al. 1971
12039,3	coarse-grained basalt/gabbro	merrillite occurs in black breccia; re-analyzed at WU	EMP	Keil et al. 1971
12013,14	KREEP-rich, granite-bearing breccia		EMP	Quick et al. 1981
15475,125	Coarse-grained basalt	Fe- and Sr-rich; re-analyzed at WU	EMP	Brown et al. 1972
65903,17-10	poikilitic impact-melt breccia	analyzed at WU	EMP	Korotev et al. 1997
73216,38	impact breccia	re-analyzed at WU	EMP	Neal et al. 1990
76503,7025	impact breccia with monzogabbro clast	merrillite occurs in composite grains with apatite and monazite	EMP	Jolliff 1993
LAP022x meteorite	coarse-grained low-Ti basalt	merrillite occurs in three compositionally distinct groups	EMP	Zeigler et al. 2005
martian				
ALH84001	coarse-grained orthopyroxenite	contains secondary carbonates	EMP	Greenwood et al. 2003
Los Angeles	shergottite basalt	merrillite occurs in the basalt mesostasis	EMP	Greenwood et al. 2003
EETA79001	shergottite basalt with multiple lithologies	merrillite occurs in the basalt mesostasis	EMP	Wang et al. 2004
Shergotty	Type shergottite (clinopyroxene-rich basalt)	merrillite occurs in the basalt mesostasis	EMP, SIMS	Lundberg et al 1988
meteoritic				
Springwater	pallasite (stony-iron meteorite)	merrillite occurs in the silicate portion of the meteorite	EMP, SIMS	Davis and Olsen 1991

accurately, the error in stoichiometry introduced by the REE measurements are small compared to uncertainties related simply to the measurement of Ca and P.

A second source of error relating specifically to REE-rich lunar merrillite has to do with matrix corrections for the electron-microprobe analyses. It is impractical to measure all of the REEs directly using the electron microprobe. However, if only a few are measured and the rest are estimated by interpolation and extrapolation, the initial electron microprobe data must be reprocessed using a full matrix correction based on the complete mineral composition. In the case of lunar merrillite, omitting the correction leads to low P and high Ca. In the average case, where the sum of (Y+REE)₂O₃ is 10–11 wt%, omitting all except Ce₂O₃ and Y₂O₃ equates to a tetrahedral cation sum that is too low by ~0.05 atoms per 56 O. If the analysis includes Y, La, Ce, Nd, Sm, and Gd, the matrix correction is minor. In some cases (e.g., Keil et al. 1971; Jolliff et al. 1993), the correction is documented, but in most analyses, it is not stated or not attempted, and may contribute to poor stoichiometry when we estimate the full REE complement.

Last, the presence of F has a significant effect on stoichiometry calculated on the basis of charge balance. For example, a 0.5 wt% content of F corresponds to a response (decrease) of about 0.07 atoms in the tetrahedral cation sum.

Given the potential for combined uncertainties in lunar merrillite analyses, we conclude that a measure of good stoichiometry is to have the sum of tetrahedral cations (P+Si) between ~13.9 and 14.1. Among the compositions listed in Table 3, two exceed 14.1, and two are less than 13.9. As the tetrahedral sum decreases

below 13.9, we consider the composition to be increasingly suspect, either in terms of low P or high Ca and/or REE sums, failure to do a full matrix correction, or the possibility that some other substituent for Ca (e.g., Sr) or for P (e.g., S) is missing from the analysis.

Samples

We list average compositions for six samples from Apollo 14 rocks reported by Jolliff et al. (1993) because those analyses included determinations of the REEs by ion microprobe, in addition to the more abundant REEs by electron microprobe. For compositions determined with the electron microprobe, it is usually possible to obtain concentrations for the abundant REE, including Y, La, Ce, Nd, Sm, Gd, Dy, Er, and possibly Yb in merrillite in lunar materials. However, rarely are these all measured, and as a check on accuracy and to analyze accurately the HREE, it is necessary to have ion-microprobe analyses. Using the relationship mentioned above for Y, we have confidence from the ion-microprobe data that chondrite-normalized values should place Y at about the same level as Ho and Er (Jolliff et al. 1993). Thus, when we have only electron-probe data, we use Y to help constrain the HREE concentrations. This constraint is important to compute the total REE concentration to assess stoichiometry. Given the typical shape and trend of chondrite-normalized lunar merrillite REE patterns known well from ion-microprobe analyses, we can interpolate or extrapolate from electron-microprobe analyses to obtain useful estimates of the less abundant REE such as Pr, Tb, Ho, Tm, and Lu and even the more abundant of the HREE including Gd, Dy, Er, and Yb.

TABLE 3. Merrillite compositions

	Lunar Rocks										
	14161, ,7350	14161, ,7373	14161, ,7044	14161, ,7264	14161, ,7233	14161, ,7069	10085 LR No. 1	12036 ,9	12039 ,3	12013 ,14	15475 ,125
Oxide concentrations (wt%)											
P ₂ O ₅	42.9	42.7	42.7	43.3	42.3	41.9	43.9	42.5	42.6	43.0	41.7
SiO ₂	0.22	0.13	0.31	0.43	0.28	0.59	0.44	0.54	0.78	0.21	0.28
Al ₂ O ₃	<0.02	<0.02	<0.02	<0.02	<0.02	<0.02	0.22	0.25	0.12	0.00	na
FeO	0.13	1.96	0.86	1.00	0.47	3.47	0.95	2.13	1.23	1.30	5.85
MnO	0.01	0.06	0.02	0.03	0.02	0.09	0.06	nr	nr	<0.02	0.03
MgO	3.55	2.55	3.18	3.18	3.35	1.57	3.26	3.80	3.20	2.91	0.55
CaO	39.6	41.1	40.5	40.0	40.6	38.8	40.6	42.3	41.9	39.0	39.2
SrO	na	na	na	na	<0.05	na	nr	na	na	0.04	0.26
Na ₂ O	0.19	0.53	0.58	0.36	0.53	0.18	0.77	0.33	0.37	0.12	0.06
Y ₂ O ₃	3.05	2.58	2.88	2.92	2.85	3.85	2.74	2.28	2.97	3.10	2.13
La ₂ O ₃	1.24	0.83	0.86	1.09	0.87	1.12	0.93	0.50	0.79	1.21	1.01
Ce ₂ O ₃	3.28	2.32	2.39	2.84	2.33	2.82	2.35	1.69	2.03	3.22	2.93
Pr ₂ O ₃	0.424	0.295	0.302	0.358	0.288	0.355	0.31	0.30	0.41	0.40	0.40
Nd ₂ O ₃	2.033	1.387	1.456	1.625	1.357	1.610	1.96	1.04	1.22	1.9	1.91
Sm ₂ O ₃	0.521	0.362	0.412	0.441	0.346	0.437	0.35	0.26	0.32	0.5	0.399
Eu ₂ O ₃	0.004	0.006	0.004	0.003	0.006	0.003	na	na	na	na	na
Gd ₂ O ₃	0.486	0.377	0.423	0.452	0.379	0.451	0.32	0.50	0.28	0.93	0.346
Tb ₂ O ₃	0.079	0.063	0.071	0.075	0.066	0.074	0.064	0.060	0.057	0.186	0.059
Dy ₂ O ₃	0.488	0.399	0.456	0.507	0.462	0.503	0.42	0.37	0.41	1.228	0.365
Ho ₂ O ₃	0.097	0.083	0.097	0.105	0.092	0.104	0.089	0.070	0.070	0.260	0.074
Er ₂ O ₃	0.247	0.215	0.250	0.271	0.256	0.269	0.24	0.18	0.18	0.210	0.175
Tm ₂ O ₃	0.030	0.026	0.033	0.037	0.039	0.036	0.033	0.017	0.020	0.096	0.023
Yb ₂ O ₃	0.168	0.145	0.183	0.215	0.222	0.197	0.214	0.07	0.16	0.17	0.132
Lu ₂ O ₃	0.021	0.018	0.021	0.027	0.022	0.027	0.026	0.013	0.016	0.076	0.015
F	0.15	0.12	0.14	0.11	0.13	0.08	0.07	nr	nr	0.6	<0.3
Total	98.9	98.3	98.1	99.4	97.3	98.5	100.4	99.2	99.1	100.6	100.6
- O ≡ F	0.06	0.05	0.06	0.05	0.05	0.03	0.03	0.05	0.00	0.25	0.13
Total	98.9	98.2	98.1	99.3	97.2	98.5	100.4	99.2	99.1	100.4	100.5
Y+REE ₂ O ₃	12.16	9.11	9.83	10.97	9.59	11.85	10.04	7.35	8.93	13.47	12.36
Cations per 56 O atoms											
P	13.90	13.87	13.85	13.90	13.98	13.83	13.87	13.50	13.58	14.04	13.86
Si	0.084	0.052	0.119	0.163	0.108	0.229	0.165	0.203	0.294	0.081	0.110
Sum (P,Si)	13.98	13.92	13.97	14.06	14.08	14.06	14.03	13.70	13.87	14.12	13.97
Al	<0.015	<0.015	<0.015	<0.015	<0.015	<0.015	0.098	0.188	0.090	0.000	0.000
Fe ⁺²	0.042	0.630	0.276	0.317	0.149	1.128	0.296	0.668	0.387	0.419	1.921
Mn ⁺²	0.004	0.020	0.007	0.010	0.006	0.028	0.019	0.000	0.000	0.000	0.010
Mg	2.026	1.457	1.815	1.795	1.893	0.907	1.810	2.125	1.796	1.673	0.322
Ca	16.25	16.87	16.61	16.23	16.47	16.04	16.23	17.00	16.90	16.11	16.49
Sr	na	na	na	na	<0.001	na	nr	na	na	0.009	0.059
Na	0.140	0.396	0.427	0.263	0.391	0.136	0.559	0.240	0.270	0.090	0.046
partial sum	18.46	19.37	19.14	18.61	18.90	18.24	19.01	20.22	19.45	18.30	18.84
Y+REE	1.86	1.41	1.53	1.67	1.47	1.90	1.51	1.13	1.40	1.90	1.54
Sum Cations	20.32	20.78	20.67	20.28	20.38	20.13	20.52	21.35	20.85	20.20	20.39
F	0.008	0.006	0.007	0.006	0.007	0.004	0.004	0.000	0.000	0.032	<0.016

Notes: na = not analyzed; nr = not reported. Values in italics determined by interpolation or extrapolation.

References: All 14161,7xxx samples from Jolliff et al. 1993. Each composition represents an average of all individual spot analyses from each of the 6 samples. 10085 "Lunary rock" is an average of three analyses from "LR No. 1" given by Albee and Chodos 1970. 12036,9 and 12039,3 = Keil et al. 1971. Rock 12013 = Quick et al. 1981, and Washington University (WU) EMP. 15475 = WU EMP.

We include several lunar merrillite samples from other landing sites and different rock types to explore the range of compositional variability. Sample 10085 is a shocked Ti-rich rock with basaltic mineralogy that was studied by Albee and Chodos (1970). They presented three analyses of "whitlockite" in "Lunary Rock No. 1" that are very similar to each other, and we present an average of these in Table 3, with an estimate by extrapolation of the REE that were not measured. Apollo 12 samples 12036 and 12039 are coarse-grained basaltic/gabbroic rocks. Rock 12036 contains cumulus olivine, pigeonite, augite, plagioclase, and Cr-spinel, with K-feldspar, baddeleyite, metallic Fe, apatite, and merrillite found in the intercumulus regions. Rock 12039 contains plagioclase, augite, and pigeonite, with pyroxene zoned to pyroxferroite. The assemblage also contains ilmenite, ulvöspinel, troilite, native Fe, and silica phases, in addition to Ca phosphate.

Merrillite in Apollo 12 sample 12013 was analyzed by Quick

et al. (1981). This rock is a large KREEP-rich, partly felsic (granitic) and partly black breccia delivered to the Apollo 12 site by impact (Albee et al. 1970). Quick et al. measured merrillite in the black breccia. The two analyses listed by Quick et al., measured with the electron microprobe, lacked values for Y and gave unusual values for Ca, P, and Er. We obtained a thin section of this rock, 12013,14, and found its merrillite to be similar in composition for most elements to those reported by Quick et al.

The composition of merrillite in Apollo 15 basalt 15475 was reported by Brown et al. (1972). It caught our attention because it is relatively rich in Fe and Sr; however, several key elements were omitted from the early analysis so we obtained a thin section (15475,125) and reanalyzed it. Our analysis confirmed the Fe and Sr values, but our measured REE concentrations were significantly higher.

Sample 65903,17-10 was analyzed in our lab; this is a small

TABLE 3.—Continued

	Lunar Rocks						Martian Meteorites				Pallasite
	65903	73216	76503	LAP022xx Lunar Meteorite			ALH	Los	EETA	Shergotty	Spring-
	,17-10	,38	,7025	Group 1	Group 2	Group 3	84001	Angeles	79001		water
	Oxide concentrations (wt%)										
P ₂ O ₅	42.4	43.9	42.4	43.7	42.6	38.0	46.0	44.9	45.6	44.4	46.9
SiO ₂	0.61	0.17	0.32	0.65	0.59	2.67	0.07	0.105	0.1	0.12	0.026
Al ₂ O ₃	na	na	na	0.02	0.03	0.02	nr	nr	<0.02	0.031	0.003
FeO	1.10	0.72	1.54	6.65	6.41	6.62	0.78	4.955	4.97	4.21	0.913
MnO	0.04	0.00	0.09	0.07	0.09	0.02	nr	nr	<0.04	0.16	0.027
MgO	3.01	3.25	2.69	0.20	0.2	0.05	3.53	0.91	1.25	1.44	3.61
CaO	40.5	41.3	38.8	42.8	39.7	34.2	46.5	46.9	46.2	46.2	47.3
SrO	na	0.04	0.03	0.20	0.28	0.21	nr	nr	0.02	<0.05	nr
Na ₂ O	0.46	0.44	0.03	0.17	0.039	0	2.45	1.2	0.72	1.27	2.5
Y ₂ O ₃	2.54	1.96	3.42	1.82	2.929	4.783	na	na	0.136	0.100	0.0262
La ₂ O ₃	1.01	0.77	1.24	0.50	1.025	2.147	na	na	bdl	0.020	0.0076
Ce ₂ O ₃	2.55	2.48	3.32	1.45	2.70	4.84	na	na	0.127	0.048	0.0170
Pr ₂ O ₃	0.35	0.24	0.45	0.20	0.37	0.66	na	na	na	0.006	0.0032
Nd ₂ O ₃	1.53	1.22	2.14	0.91	1.68	2.71	na	na	bdl	0.034	0.0192
Sm ₂ O ₃	0.70	0.51	0.70	0.27	0.46	0.70	na	na	bdl	0.012	0.0060
Eu ₂ O ₃	na	na	na	na	na	na	na	na	na	0.003	0.0003
Gd ₂ O ₃	1.10	0.56	1.10	0.41	0.77	1.10	na	na	bdl	0.016	0.0049
Tb ₂ O ₃	0.175	0.055	0.175	0.065	0.122	0.175	na	na	na	0.003	0.0007
Dy ₂ O ₃	0.80	0.34	0.80	0.37	0.70	1.00	na	na	na	0.021	0.0050
Ho ₂ O ₃	0.098	0.067	0.132	0.070	0.113	0.184	na	na	na	0.004	0.0009
Er ₂ O ₃	0.18	0.12	0.24	0.14	0.21	0.33	na	na	na	0.012	0.0022
Tm ₂ O ₃	0.016	0.140	0.016	0.016	0.024	0.030	na	na	na	0.002	0.0003
Yb ₂ O ₃	0.05	0.11	0.05	0.07	0.11	0.11	na	na	bdl	0.009	0.0021
Lu ₂ O ₃	0.004	0.011	0.004	0.008	0.013	0.010	na	na	na	0.001	0.0003
F	<0.3	0.5	0.47	0.51	0.37	0.46	0	0	<0.3	0	nr
Total	100.1	98.9	100.2	101.5	101.5	101.0	99.3	99.0	99.7	98.1	101.4
- O ≡ F	0.21	0.20	0.21	0.16	0.19	0.00	0.00	0.17	0.00		
Total	99.7	98.7	100.0	101.3	101.4	100.8	99.3	99.0	99.5	98.1	101.4
Y+REE ₂ O ₃	11.10	8.58	13.79	6.30	11.22	18.77	na	na	<0.4	0.29	0.10
	Cations per 56 O atoms										
P	13.70	14.01	13.81	13.84	13.77	12.92	14.01	13.99	14.11	13.95	14.02
Si	0.234	0.064	0.122	0.243	0.225	1.072	0.025	0.039	0.037	0.045	0.009
Sum (P,Si)	13.93	14.08	13.93	14.09	14.00	13.99	14.04	14.03	14.14	13.99	14.03
Al	0.000	0.000	0.000	0.008	0.011	0.000	0.000	0.000	0.000	0.014	0.001
Fe ⁺²	0.350	0.227	0.494	2.079	2.049	2.224	0.235	1.525	1.520	1.306	0.269
Mn ⁺²	0.012	0.000	0.030	0.022	0.029	0.007	0.000	0.000	0.000	0.050	0.008
Mg	1.714	1.827	1.542	0.111	0.114	0.030	1.894	0.499	0.681	0.796	1.899
Ca	16.541	16.70	15.98	17.15	16.26	14.72	17.93	18.49	18.11	18.35	17.88
Sr	0.000	0.009	0.007	0.043	0.062	0.049	0.000	0.000	0.004	0.000	0.000
Na	0.337	0.322	0.024	0.125	0.029	0.000	1.709	0.856	0.510	0.913	1.711
partial sum 1	18.95	19.08	18.08	19.54	18.55	17.03	21.77	21.38	20.83	21.43	21.77
Y+REE	1.66	1.28	2.11	0.95	1.71	3.02	na	na	0.06	0.04	0.01
Sum Cations	20.62	20.36	20.19	20.49	20.27	20.05	21.77	21.38	20.89	21.47	21.79
F	<0.016	0.026	0.025	0.027	0.019	0.024	<0.02				

Notes: na = not analyzed; nr = not reported; bdl = below detection limit. Values in italics determined by interpolation or extrapolation. References: 65903,17-10 = Zeigler et al. 2005; 73216,38 = Neal et al. 1990; 76503,7025 = Jolliff 1993; LAP022xx Lunar meteorite = Zeigler et al. 2005; martian meteorites ALH84001 (average of 4 reported compositions) and Los Angeles (average of two reported compositions) = Greenwood et al. 2003; EETA79001, TS357,1720 = WU EMP (total REE estimated from Ce, Y); Shergotty = Lundberg et al. 1988; Springwater Pallasite = Davis and Olsen 1991.

rock fragment of a clast-poor, poikilitic impact melt-breccia from Apollo 16 soil (Korotev et al. 1997). Neal et al. (1990) listed compositions of merrillite in different lithologies of Apollo 17 impact breccia 73216 but omitted Si. We obtained a thin section of 73216,38 and found merrillite of similar but not identical composition, which is given in Table 3.

The three groups listed under the heading of LAP022xx are from the LaPaz Icefield basaltic lunar meteorite, which was described by Zeigler et al. (2005). This rock is unusual in that we found three distinct groups of merrillite according to their REE concentration levels, and one of these levels is exceptional for lunar merrillite. The values listed in Table 3 are averages of several measurements of grains in each group.

We include four compositions of merrillite in martian meteorites. One of these, from Shergotty, a clinopyroxene-rich basalt, includes ion-microprobe data (Lundberg et al. 1988).

We analyzed EETA79001, a multi-lithology shergottite basalt, in our lab as part of a broad study of this meteorite, e.g., Wang et al. (2004). Our thin section, no. 357,1720, derives from the homogeneous basalt lithology (see Meyer 1996). Two compositions, which are averages of analyses of grains in ALH84001 and Los Angeles, are included from Greenwood et al. (2003); these help to illustrate the range of Na in the martian materials. ALH84001 is a cataclastic orthopyroxenite, known for its magnetite and Ca-Fe-Mg carbonate, and Los Angeles is a chemically, relatively evolved shergottite basalt. Even though REE concentrations were not analyzed directly in the ALH84001 and Los Angeles merrillite grains, it is clear from the analyses that REE concentrations must be relatively low.

Last, we include a composition of merrillite from the Springwater pallasite analyzed by Davis and Olsen (1991). This is a stony-iron meteorite in which phosphates crystallized from

silicate portions of melt on the meteorite's planetary body. Davis and Olsen interpreted Springwater to have come from relatively shallow depth in the differentiating parent-body mantle where trace-element contents of the merrillite reflect late-stage crystallization of melt. There are many published analyses of meteoritic merrillite, and they range from Ca-rich [e.g., Estacado (Prewitt and Rothbard 1975) and Angra dos Reis (Dowty 1977)] to Na-rich (Springwater). The composition given for the Springwater pallasite is one of the few published compositions that includes Si and Na, in addition to the usual major elements, and also includes the REEs determined with the ion microprobe.

RESULTS

Compositions

Smith and Steele (1976) provided an excellent summary of lunar merrillite compositions. Here, we update the summary and provide additional merrillite compositions (Table 3). We then discuss substitutions and systematic compositional variations in this very interesting mineral.

Many elements have been listed as constituents in extraterrestrial merrillite, and we will surely not list them all here. The main or "essential" elements that occur in the various end-members, in addition to Ca and P, include Mg, Fe, Na, and Y+REE. Magnesium and Fe are always present at around 2 atoms per 56 O, and the natural samples cover a range of Mg/(Mg + Fe) atomic from 0.98 (14161,7350) to 0.01 (LAP Gp3). These levels correspond to ~3.8 wt% MgO and 6.6 wt% FeO, respectively. The most Fe-rich compositions occur in basalts and correspond to the extent of Fe-enrichment attained by the final trapped-melt component. Jolliff et al. (1993, their Fig. 7) showed that merrillite is more magnesian than coexisting apatite and mafic silicates except in the most extreme cases of Fe enrichment when Fe/(Mg + Fe) values converge to 1. Manganese, which is commonly associated with Fe and Mg, occurs in relatively low concentrations, ranging from near zero to 0.16 wt%. It is of note that there is an Mn-rich (terrestrial) whitlockite end-member (Kostiner and Rea 1976). In the lunar assemblages where mer-

rillite occurs, however, pyroxene is always present and competes well for available Mn.

In the lunar materials, the Y+REE concentrations are high in nearly all samples measured to date and are higher than in coexisting apatite and the main silicate minerals (Fig. 3). All lunar merrillite compositions listed in this paper have greater than 6 wt% Y+REE as oxides, average about 8–10 wt%, and range up to nearly 19 wt%. These concentrations correspond to a range of ~1 to 3 atoms per 56 O. The average of the samples listed in Table 3 is ~1.5 and most do not exceed 2 atoms per 56 O. By the number of atoms, Y is always the most abundant, typically accounting for about a third of the Y+REE atoms. By mass, Ce and Y are usually similar in concentration, each ranging from about 1.5 to 4.8 wt% as oxides. After Ce, the REE elements Nd, La, Dy, and Gd are the most abundant in terms of concentration.

In the martian meteorites, concentrations of the REE in merrillite appear to be much lower than in lunar samples. Harvey et al. (1993) and Wadhwa et al. (1994) reported REE concentrations in shergottite meteorites including Shergotty, Zagami, EETA79001 (lithologies A and B), ALHA77005, and LEW88516. Of these, the highest concentrations are less than 0.3 wt% total RE₂O₃ (including Y₂O₃, approximated from the HREE). These low concentrations are consistent with the compositions listed in Table 3.

Concentrations of Si and Na are very important in extraterrestrial merrillite, even if low, because these are the main ions involved in providing charge balance for the substitution of trivalent REE for divalent Ca. In the samples of Table 3, Si ranges from near zero to 2.67 wt%, and Na ranges from zero to 0.77 wt% in the lunar samples. These maximum values correspond to 1.07 Si per 56 O and 0.56 Na per 56 O. This number of Na atoms corresponds to about one quarter filling of the available Na sites.

Strontium, although not typically reported, is present in significant concentrations, e.g., 0.2–0.3 wt% in LAP and 15475 merrillite (Table 3), and was reported as high as 1 wt% in another sample of 15475 (Brown et al. 1972). Barium and K have been also reported, but only at about the 0.05 wt% level (Albee and Chodos 1970). These concentrations are probably very near the detection limits in routine electron-microprobe analyses, and we did not include K and Ba in our wavelength-dispersive analyses of merrillite.

Aluminum is typically found in low concentrations, ranging from near zero to 0.25 wt% (as Al₂O₃). However, these values may be significant, and Al should be measured in merrillite analyses. The sample in Table 3 that has the highest Al concentration also has the lowest P+Si total (12036.9). If Al substitutes on tetrahedral sites, it would improve the stoichiometry of this sample considerably and would provide a potential double-charge balance if substituting for P⁵⁺.

The halogens (F and Cl) are commonly reported in lunar merrillite analyses, although their concentrations are typically low. We have not detected Cl in any of our own analyses by electron microprobe. Fluorine, which was discussed in the section on analytical methods, may be misreported in some of the published literature in cases where the third-order P peak was mistaken for F. Greenwood et al. (2003) found no F in the

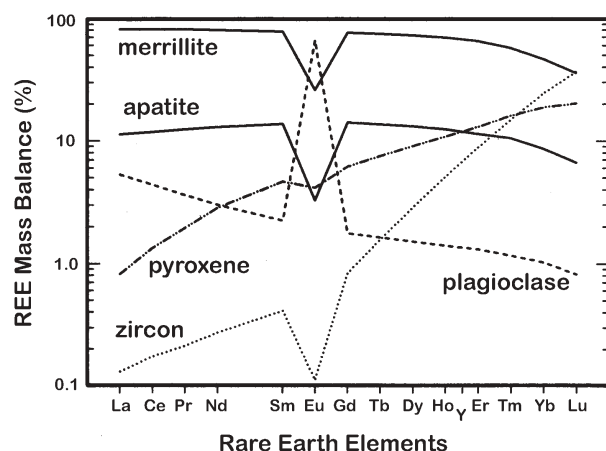


FIGURE 3. Relative distribution (mass balance) of Y+REE in minerals typically occurring in an assemblage with lunar merrillite (after Jolliff et al. 1993). (N.B. These are not mineral/melt distribution coefficients.)

martian merrillite in ALHA84001 and Los Angeles. Although we show F concentrations in Table 3, we are wary of the fact that many of these concentrations are at or near the detection limit of our analyses (under routine conditions, about 0.3 wt%). Moreover, some merrillite grains, especially very small ones, appear susceptible to beam damage, so F may volatilize or migrate during an analysis. However, we have repeatedly made wavescans across the F peak position and we almost always find a bump over background to convince us that low concentrations up to about 0.5 wt% in lunar merrillite are real.

We and most others have not routinely analyzed for S in merrillite; however, it is a possible substituent for P in phosphates such as apatite and merrillite. We have analyzed for S in several instances, and we find its concentration to be near the detection limit using the electron microprobe (0.0x wt%). However, low concentrations—on the order of 0.05 to 0.1 wt%—are confirmed by wavescans across the S peak. A concentration of 0.1 wt% S as SO_3 contributes ~ 0.03 cations per 14 tetrahedral cations. We suspect that higher concentrations are possible and thus S should be considered when tetrahedral cation sums are low.

Finally, we note that the actinides U and Th have been reported in merrillite as well as in coexisting apatite. Quick et al. (1981) reported 0.18 and 0.08 wt% ThO_2 in merrillite grains from 12013; however, these levels are very difficult to measure with the electron microprobe using $M\alpha$ lines. Crozaz et al. (1989)

tabulated U concentrations in apatite and merrillite in chondritic meteorites and showed that enrichment favors apatite by factors ranging from ~ 1.5 to 27 and mostly in the range of 10–20.

Raman spectra

Raman spectra of lunar REE-merrillite, synthetic REE-rich and REE-poor merrillite, and terrestrial whitlockite were reported by Jolliff et al. (1996). Merrillite and whitlockite, and other phosphates such as apatite, have strong and distinctive Raman spectra (Fig. 4) (see also Cooney et al. 1999). All of these spectra have prominent Raman peaks due to vibrations within the phosphate tetrahedra. In merrillite and whitlockite, the strongest bands in the 950–975 Δcm^{-1} region are associated with the ν_1 symmetric-stretching vibration of the phosphate group. Other features shared by all of the spectra include weak bands in the 1080–1100 Δcm^{-1} region (ν_3 asymmetric-stretching vibration), in the 400–500 Δcm^{-1} region (ν_2 bending mode), and in the 550–660 Δcm^{-1} region (ν_4 bending mode). Weak bands at less than 400 Δcm^{-1} are lattice modes. In the terrestrial H-bearing whitlockite and the REE-poor synthetic Ca-merrillite (Figs. 4a and 4c), the strong ν_1 band is a well-resolved doublet, as it is also in “Na-whitlockite” of the Sixiangkou chondrite (Chen et al. 1995) and in merrillite in ALH84001 (Cooney et al. 1999). However, in lunar REE-merrillite and REE-rich synthetic merrillite, this band is an asymmetric single peak and a very poorly resolved

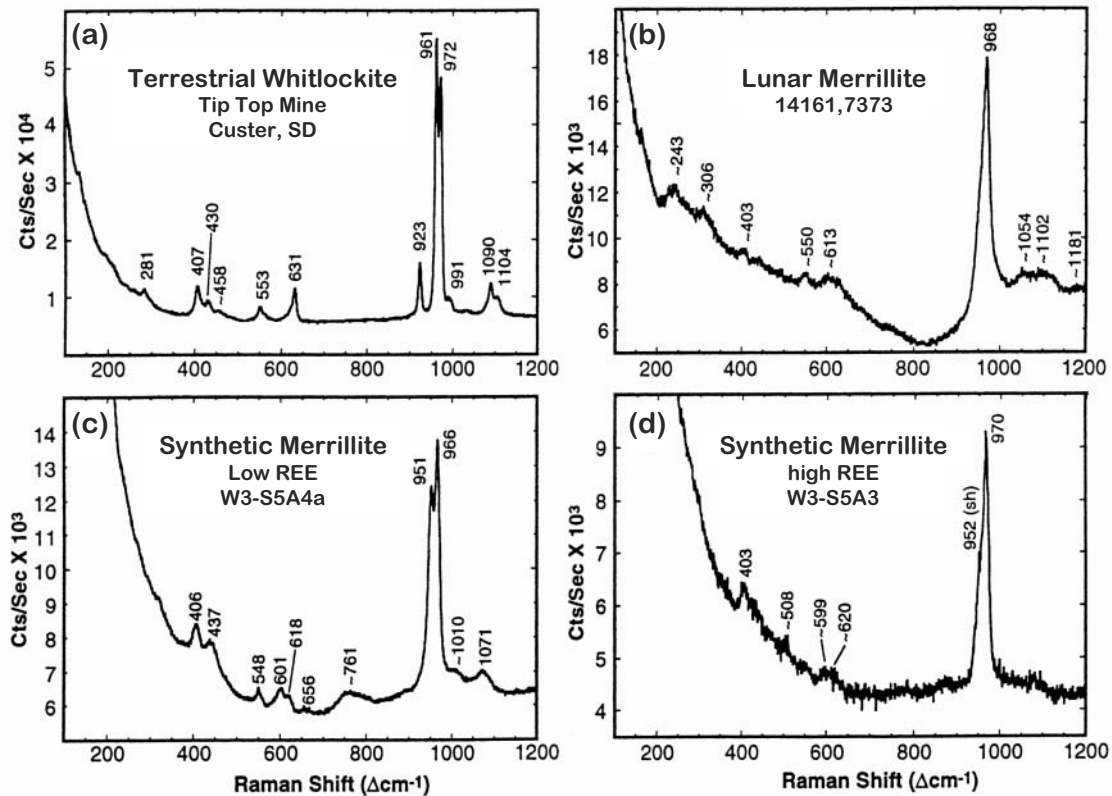


FIGURE 4. Raman spectra of whitlockite and merrillite (a) Terrestrial whitlockite from the Tip-Top pegmatite, South Dakota, with a well-resolved doublet at 961 and 972 Δcm^{-1} , and a third ν_1 band at 923 Δcm^{-1} . (b) Lunar REE-whitlockite from sample 14161,7373 (Jolliff et al. 1993; Hughes et al. 2006), with single, asymmetric band at 968 Δcm^{-1} . (c) Synthetic REE-poor whitlockite (Colson and Jolliff 1993), with well-resolved doublet at 951 and 966 Δcm^{-1} . (d) Synthetic REE-rich whitlockite (Colson and Jolliff 1993), with single band at 970 Δcm^{-1} and weak shoulder at 952 Δcm^{-1} .

doublet, respectively (Figs. 4b and 4d). Terrestrial whitlockite has an additional weak peak at 923 cm^{-1} that is not observed in the spectra of the H-free merrillite; we attribute this to the ν_1 mode of HPO_4^{2-} groups involving P1 (PA') tetrahedra. In general, Raman bands of hydroxyl ions occur as sharp, well-defined bands at or above 3200 cm^{-1} . However, the Raman-active O-H stretch of the weakly acidic hydroxyl group in HPO_4^{2-} is likely to be broad and very weak, located in the $2100\text{--}2700 \text{ cm}^{-1}$ region of the vibrational spectrum. We did not locate this band in the terrestrial whitlockite sample, possibly because of the weak background fluorescence observed in this spectral region.

In addition to the Raman bands discussed above, Jolliff et al. (1996) observed an increased background in the region from $\sim 1000\text{--}1500 \text{ cm}^{-1}$ in the lunar REE-merrillite spectrum (only partially seen in Fig. 4b). We attribute this primarily to the laser-induced fluorescence of Er^{3+} . The Er^{3+} ion has transitions low enough in energy to be excited by the 514 nm line of the Ar-ion laser. This increased background was not observed in the spectra of synthetic merrillite grains that do not contain Er (Jolliff et al. 1996).

Using Raman spectroscopy, we thus can distinguish between whitlockite that has essential (i.e., structurally necessary) H from totally anhydrous merrillite, which is consistent with the X-ray structural analysis. In the case of the anhydrous merrillite, the Raman spectrum also reflects a significant structural difference between REE-rich and REE-poor merrillite, as follows. The well-resolved doublet in the terrestrial whitlockite, the meteoritic Na-whitlockite (Chen et al. 1995), and the REE-poor synthetic merrillite reflects at least two types of symmetrically distinct phosphate groups that are subject to different local bonding environments. These may correspond to P(B1) and P(B2) distinguished by X-ray refinement (Dowty 1977). The spectrum of the terrestrial whitlockite from the Tip Top mine is nearly identical to that of the Sixiangkou whitlockite (Chen et al. 1995) except for the peak at 923 cm^{-1} found only in the former. The spectra of the lunar and synthetic REE-rich merrillite samples, however, do not exhibit the well-resolved ν_1 doublet, suggesting that the coupled substitution of REE^{3+} for Ca^{2+} in Ca(B) sites and the creation of vacancies on Ca(IIA) sites result in a more uniform bonding environment for all phosphate groups. The synthetic REE-whitlockite has a slight shoulder at 952 cm^{-1} even though it has a higher total REE concentration than the lunar sample (Table 4). However, the synthetic sample is dominated by light REE, whose effective ionic radii are closer to that of Ca^{2+} , whereas the lunar sample also has high concentrations of heavy REE including Y, which are progressively smaller than Ca^{2+} . Thus we are not surprised to find a more pronounced structural change in the lunar REE-merrillite, even though it has a lower total REE

concentration than the synthetic one (Table 4). We observe the same Raman spectral features and elevated fluorescence background in merrillite grains in other lunar samples.

The Raman spectra support the contention of Calvo and Gopal (1975), Prewitt and Rothbard (1975), Dowty (1977), and Hughes et al. (2006, this issue) that H-free varieties of merrillite, including lunar REE-merrillite, have structural differences from terrestrial whitlockite that lead to significantly different crystal-chemical behavior thus justifying the name *merrillite*. In particular, the Raman spectra of terrestrial whitlockite contain a peak at 923 cm^{-1} interpreted as resulting from an HPO_4^{2-} group that is missing in lunar and martian merrillite analyzed to date, and in synthetic merrillite.

DISCUSSION

Compositional variations

In lunar merrillite, the main compositional variable is its REE content. The concentrations range from about 1 to 3 atoms per 56 O. Notably, the extremes in terms of the samples listed in Table 3 occur in a single sample (the LAP lunar basaltic meteorite). This observation is significant with respect to petrologic understanding of the variation of REE concentrations in lunar merrillite. The level of concentration does not reflect the petrologic evolution of the rock that hosts the merrillite, instead it simply reflects the state of the immediately surrounding pocket of late-stage residual melt from which the merrillite crystallized. Smith and Steele (1976) also came to this conclusion. In fact, among the Apollo 14 specimens listed in Table 3, 14161,7233 and 14161,7373 whole-rock samples have among the highest REE concentrations of any known lunar materials (Jolliff 1991, Jolliff et al. 1999), but their merrillite grains have among the lowest REE concentrations. The concentrations of the REE in merrillite ultimately depend on the F contents of residual melt and on how much apatite forms relative to merrillite. Jolliff et al. (1993) drew on this relationship to show how the coexisting apatite and merrillite grains in a given rock could form with the observed, but variable, REE concentration ratios simply as a function of the proportions of the two minerals within residual melt pockets as the melts approached complete crystallization.

Substitutions

An issue for this paper is how the REE are incorporated into merrillite, specifically, how charges are balanced. If there is more than one major charge-balancing coupled substitution, that might help to explain the wide range of distribution coefficients that appears to apply to lunar merrillite. Understanding the substitutional and charge-balancing relationships also aids our understanding of what sets the different suites of merrillite apart and which traits might reflect processes that are unique to their parent planet.

To investigate potential substitution relationships, we show a plot of the sum of Y+REE vs. Ca in Figure 5a. The correlation is very good, with a correlation coefficient of 0.96. The slope is -1.2 , however, not -1.5 as would be the case if the substitution was simply $(\text{Y}+\text{REE})_{2,\text{Ca site}} + \square_{\text{Na site}} \leftrightarrow \text{Ca}_3$ where \square represents a vacancy, presumably (but not necessarily) in the Na site (= CaIIA site). Adding Na to Ca, however, brings the slope to -1.5

TABLE 4. Merrillite and whitlockite formulae, Raman experiment

End-member/sample (occurrence)	Formula
Tip Top (terrestrial)	$\text{Ca}_{17.8}\text{Mg}_{1.9}\text{Na}_{0.3}\text{H}_2\text{P}_{14}\text{O}_{56}$
14161,7373 (lunar)*	$\text{Ca}_{16.8}\text{REE}_{1.4}(\text{Mg,Fe})_{2.1}\text{Na}_{0.39}\text{P}_{13.9}\text{Si}_{0.05}\text{O}_{56}$
W3-S5A3 (REE-rich, synthetic)†	$\text{Ca}_{16.6}\text{REE}_{1.8}(\text{Mg,Fe})_{1.9}\text{Na}_{0.13}\text{P}_{13.4}\text{Si}_{0.57}\text{O}_{56}$
W3-S5A4a (REE-poor, synthetic)†	$\text{Ca}_{18.7}\text{REE}_{0.05}(\text{Mg,Fe})_{2.0}\text{Na}_{0.17}\text{P}_{13.9}\text{Si}_{0.16}\text{O}_{56}$

* In the lunar sample, "REE" includes Y.

† Synthetic samples include only the elements La, Nd, Sm, and Yb. Formulae of samples were calculated on the basis of 56 O atoms. H in the Tip Top whitlockite was not measured but was taken to be present at 2 per 56 O to calculate this formula. Experimental samples from work of Colson and Jolliff (1992, 1993a).

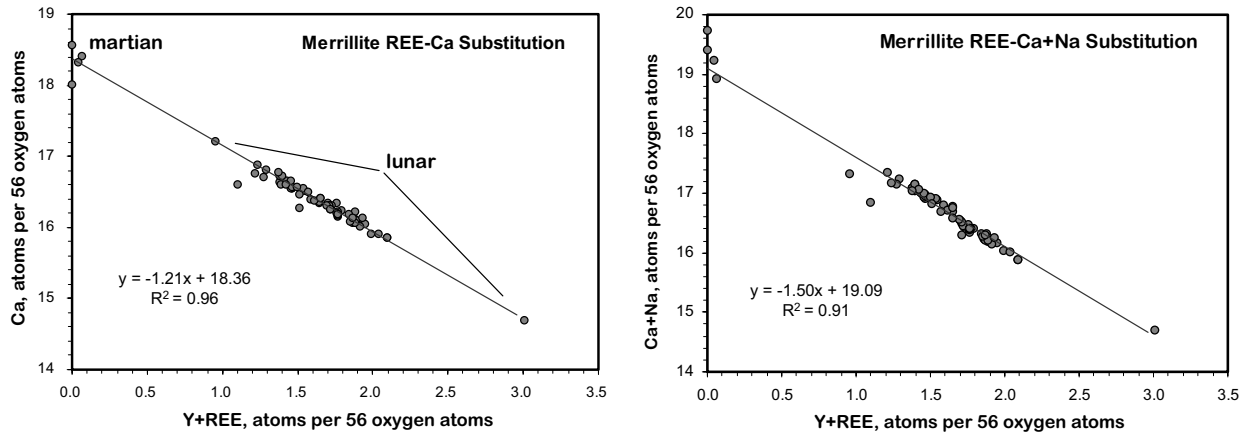


FIGURE 5. (a) Y+REE vs. Ca (atoms per 56 O atoms) in lunar and martian merrillite. Data are for the same samples as shown in Table 3 (lunar and martian) but include all of the individual spot analyses for the lunar materials. Regression equation is for the line shown fit to the lunar samples. (b) Y+REE vs. Ca+Na (atoms per 56 O atoms) in lunar and martian merrillite. Same data as in a. Regression equation is for only the lunar data points, excluding the most REE-rich outlier.

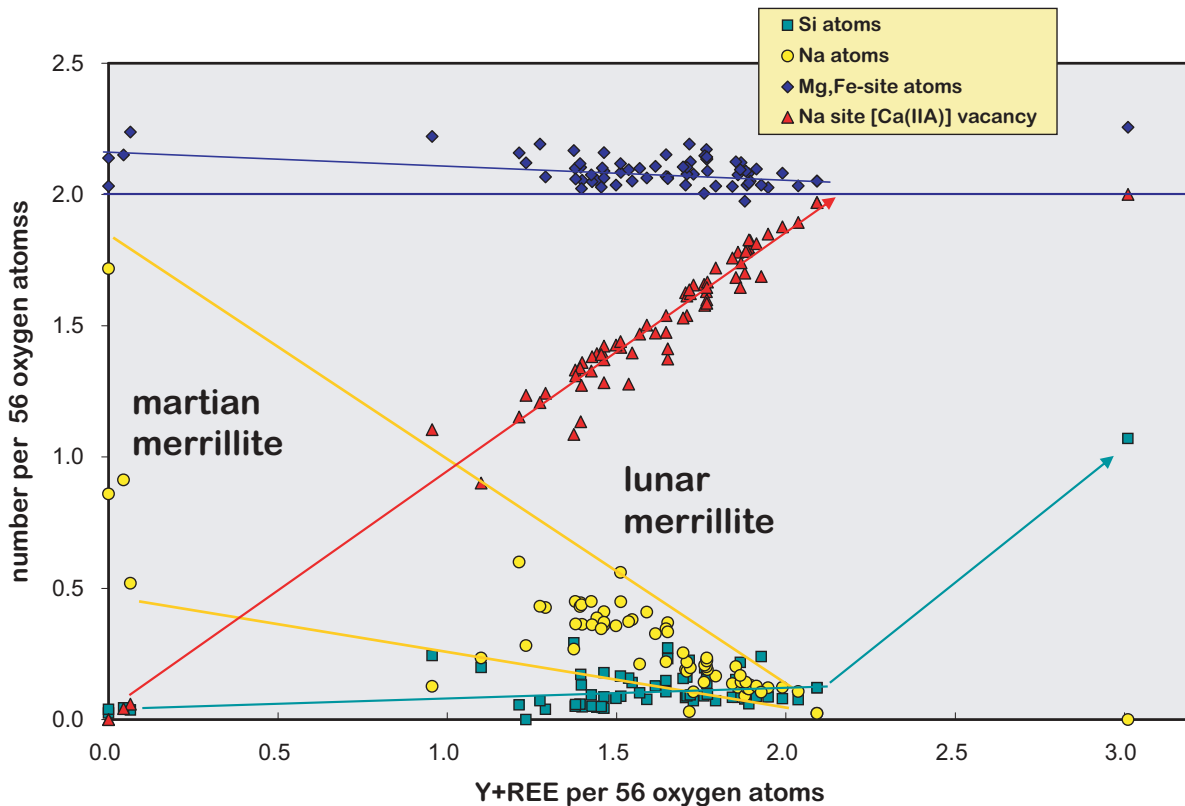


FIGURE 6. Y+REE vs. other cations in merrillite, expressed as cations per 56 O atoms. Data are for the same samples as shown in Table 3 (lunar and martian) but include all of the individual spot analyses for the lunar materials. Mg,Fe site atoms include Mg, Fe, and Mn. To plot the Na-site vacancy, stoichiometry is forced to Si + P = 14 per 56 O, and reported F concentrations are neglected. Calculated vacancy on the Na site [Ca(IIA)] increases linearly with the sum of Y+REE for values between 0 and 2 per 56 O atoms (red arrow). Because the Na site is fully vacated at 2 Y+REE atoms per 56 O atoms, further REE substitution is balanced by increasing silicon substitution for P (blue arrow extending from Y+REE=2 to Y+REE=3).

(Fig. 5b), consistent with $(Y+REE)_{2,Ca\ site} + \square_{1-2,Na\ site} \leftrightarrow Ca_{2,Ca\ site} + (Na,Ca)_{1-2,Na\ site}$. That the number of Na atoms goes to zero at 2 Y+REE is consistent with vacancy occurring primarily on the Na site and not on other Ca sites.

To determine how charges are balanced, we plot the Y+REE atoms vs. several of the notable compositional variables, including Si and Na, in Figure 6. This figure shows the decrease in Na cations as the sum Y+REE increases. Although outliers

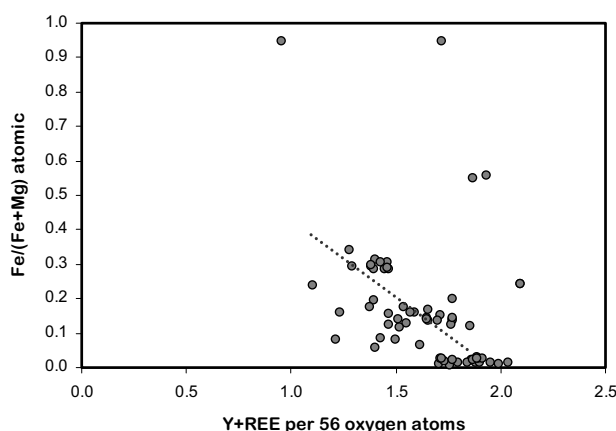


FIGURE 7. Fe/(Fe + Mg) atomic vs. Y+REE in lunar merrillite in the range of Y+REE from 1 to just over 2 atoms per 56 O. Although the data scatter, there is a trend of decreasing Fe with increasing Y+REE (see text). Dashed line is not a regression line but serves to show the inferred trend.

lie along the trend for lunar materials, especially on the low-Na side of the correlation, the general trend, indicated by the bounding yellow lines, projects to a range of Na values encompassing those of the martian samples. Vacancy on the Na site correlates well with increasing Y+REE, thus it appears that charges for REE substitution between 0 and 2 Y+REE atoms per 56 O are balanced primarily by a vacancy on the Na site, which otherwise contains Na plus some Ca (cf., Fig. 5).

Variation in the sum of Fe+Mn+Mg does correlate with increasing Y+REE, albeit weakly and with much scatter. A decrease of about 0.1–0.15 atoms per 56 O occurs as Y+REE vary over the range 0–2.2 Y+REE (Fig. 6). That the sum of Fe+Mg+Mn consistently exceeds 2 indicates some mixing of these elements on the Ca sites and possibly on the Na site as well. Colson and Jolliff (1992, 1993a, 1993b) suggested, on the basis of experimental merrillite compositions and variations, that Fe²⁺ in particular might substitute preferentially on the Na site (which they referred to as the CaIIA site) relative to the general Ca sites. Although the data scatter considerably, they do show a general trend of decrease in Fe/(Fe+Mg) with increasing Y+REE (Fig. 7), and in the general trend, Fe decreases to zero at about Y+REE = 2, consistent with the suggestion above. However, because the Fe/(Fe+Mg) ratio is primarily a function of the residual melt composition from which merrillite crystallized, this relationship is complex.

Although Si is present in all of the merrillite grains listed, its concentration varies only slightly as a function of Y+REE content over the range of 0–2 Y+REE per 56 O. The increase is consistent with the substitution $(Y+REE)_{Ca\ site}^{2+} + Si_1^{4+} \leftrightarrow Ca_{Ca\ site}^{2+} + P_1^{5+}$ accounting for only about 5% of the substitution between 0–2 Y+REE per 56 O. Above 2 Y+REE, however, one key sample, the group-3 merrillite in the LAP lunar meteorite shows an increase in Si content that corresponds almost exactly to this substitution, with a near 1:1 slope (Fig. 6). This relationship is consistent with the results of synthetic REE and Si-rich merrillite of Colson and Jolliff (1992, 1993a).

IMPLICATIONS

Extraterrestrial merrillite differs from terrestrial whitlockite by enrichments in Ca²⁺, Na⁺, or Y+REE³⁺, and the lack of H⁺. The H-free extraterrestrial varieties have a variably occupied Na site (equivalent to CaIIA of previous studies); vacancies on this site, which is otherwise partially occupied by a combination of Na and Ca, and possibly Fe²⁺, provide a favorable charge-balance for Y+REE \leftrightarrow Ca substitution in the lunar material. In martian merrillite, the Na site is largely filled by a combination of Ca+Na, and in some cases, Na approaches 2 atoms per 56 O. Concentrations of REE in martian merrillite analyzed to date are very low, suggesting a petrologic history significantly different from the Moon, where the incompatible trivalent REE are strongly enriched in melts residual to the main crystallizing phases, which include olivine, pyroxene, plagioclase, spinel, and Fe-Ti oxides, but lack minerals such as garnet that might otherwise serve as petrologic reservoirs for the REE, at least at depths sampled by lunar igneous systems to which we now have access. Whether all martian merrillite will prove to be anhydrous remains to be seen. Raman spectroscopy, which readily identifies the HPO₄²⁻ group in hydrous whitlockite, may prove to be a useful tool in searching for martian (H-bearing) whitlockite.

ACKNOWLEDGMENTS

This work was supported, in part, by NASA grant NNG04GG10G (B.L.J. through L.A. Haskin) and NSF grant EAR-0003201 to J.M.H. We thank James Greenwood and Charles Shearer for thoughtful and helpful reviews. Eric Fritzsche of the Museum of Geology at the South Dakota School of Mines and Technology kindly provided us with a sample of whitlockite from the Tip Top Pegmatite, Custer County, South Dakota. This brings us full circle since it was in the pegmatites of the Black Hills that the first author spent six memorable years under the mentorship of Jim Papike. Jim's enthusiasm extended from the pegmatites to the fascinating rocks of the Moon, and the first author inherited his enthusiasm.

REFERENCES CITED

- Albee, A.L. and Chodos, A.A. (1970) Microprobe investigations on Apollo 11 samples. Proceedings of the Apollo 11 Lunar Science Conference, *Geochimica et Cosmochimica Acta Supplement*, 1, 135–157.
- Albee, A.L., Burnett, D.S., Chodos, A.A., Haines, E.L., Hueneker, J.C., Papanastassiou, D.A., Podosek, F.A., Russ, G.P., III, and Wasserburg, G.J. (1970) Mineralogic and isotopic investigations on lunar rock 12013. *Earth and Planetary Science Letters*, 9, 137–163.
- Anders, E. and Grevesse, N. (1989) Abundances of the elements: Meteoritic and solar. *Geochimica et Cosmochimica Acta*, 53, 197–214.
- Armstrong, J.T. (1988) Quantitative analysis of silicate and oxide minerals: Comparison of Monte-Carlo, ZAF, and phi-rho-Z procedures. *Microbeam Analysis*, 23, 239–246.
- Brown, G.M., Emeleus, C.H., Holland, J.G., Peckett, A., and Phillips, R. (1972) Mineral-chemical variations in Apollo 14 and Apollo 15 basalts and granitic fractions. Proceedings of the 3rd Lunar Science Conference, 2, 141–157.
- Calvo, C. and Gopal, R. (1975) The crystal structure of whitlockite from the Palermo Quarry. *American Mineralogist*, 60, 120–133.
- Chambers, J.G., Snyder, G.A., and Taylor, L.A. (1995) Enigmatic major- and trace-element chemistry of some super-KREEPy Mg-rich highland rocks. *Lunar and Planetary Science*, XXVI, 225–226 (abstract).
- Chen, M., Wopenka, B., Xie, X., and El Goresy, A. (1995) A new high-pressure polymorph of chlorapatite in the shocked Sixiangkou (L6) chondrite (abs.). *Lunar Planetary Science* XXVI, 237–238.
- Colson, R.O. and Jolliff, B.L. (1993a) Crystal-chemistry and partitioning of REE in whitlockite. *Lunar and Planetary Science*, XXIV, 323–324 (abstract).
- (1993b) Effect of Fe concentration on REE partitioning in whitlockite. *EOS, Transactions of the American Geophysical Union*, 74, 343 (abstract).
- Colson, R.O., Jolliff, B.L., and Haskin, L.A. (1992) Inferring REE substitution reactions in lunar whitlockite. *Lunar and Planetary Science*, XXIII, 235–236 (abstract).
- Cooney, T.F., Scott, E.R.D., Krot, A.N., Sharma, S.K., and Yamaguchi, A. (1999) Vibrational spectroscopic study of minerals in the Martian meteorite ALH84001. *American Mineralogist*, 84, 1569–1576.
- Crozaz, G., Pellas, P., Bourot-Denise, M., de Chazal, S.M., Fiéni, C., Lundberg,

- L.L., and Zinner, E. (1989) Plutonium, uranium, and rare earths in the phosphates of ordinary chondrites—the quest for a chronometer. *Earth and Planetary Science Letters*, 93, 157–169.
- Davis, A.M. and Olsen, E.J. (1991) Phosphates in pallasite meteorites as probes of mantle processes in small planetary bodies. *Nature*, 353, 637–640.
- Delaney, J.S., O'Neill, C., and Prinz, M. (1984) Phosphate minerals in Euclides. *Lunar and Planetary Science*, XV, 208–209 (abstract).
- Donovan, J.J. and Tingle, T.N. (1996) An Improved Mean Atomic Number Correction for Quantitative Microanalysis. *Journal of Microscopy*, 2, 1–7.
- Dowty, E. (1977) Phosphate in Angra dos Reis: Structure and composition of the $\text{Ca}_3(\text{PO}_4)_2$ minerals. *Earth and Planetary Science Letters*, 35, 347–351.
- Dowty, E., Keil, K., and Prinz, M. (1974) Igneous rocks from Apollo 16 rake samples. *Lunar Science*, V, 174–176.
- Drake, M.J. and Weill, D.F. (1972) New rare earth standards for electron microprobe analysis. *Chemical Geology*, 10, 179–181.
- Frondel, J.W. (1975) *Lunar Mineralogy*, 323 p. John Wiley and Sons, Inc., New York.
- Fuchs, L.H. (1971) Orthopyroxene and orthopyroxene-bearing rock fragments rich in K, REE, and P in Apollo 14 soil sample 14163. *Earth and Planetary Science Letters*, 12, 170–174.
- Gay, P., Brown, M.G., and Rickson, K.O. (1970) Mineralogical studies of lunar rock 12023,10. *Earth and Planetary Science Letters*, 9, 124–126.
- Gopal, R. and Calvo, C. (1972) Structural relationship of whitlockite and $\beta\text{-Ca}_3(\text{PO}_4)_2$. *Nature Physical Science*, 237, 30–32.
- Gopal, R., Calvo, C., Ito, J., and Sabine, W.K. (1974) Crystal structure of synthetic Mg-whitlockite, $\text{Ca}_8\text{Mg}_2\text{H}_2(\text{PO}_4)_{14}$. *Canadian Journal of Chemistry*, 52, 1155–1164.
- Greenwood, J.P., Blake, R.E., and Coath, C.D. (2003) Ion microprobe measurements of O(18)/O(16) ratios of phosphate minerals in the Martian meteorites ALH84001 and Los Angeles. *Geochimica et Cosmochimica Acta*, 67, 2289–2298.
- Griffin, W.L., Åmli, R., and Heier, K.S. (1972) Whitlockite and apatite from lunar rock 14310 and from Ödegården, Norway. *Earth and Planetary Science Letters*, 15, 53–58.
- Harvey, R.P., Wadhwa, M., McSween, H.Y., Jr., and Crozaz, G. (1993) Petrography, mineral chemistry, and petrogenesis of Antarctic shergottite LEW88516. *Geochimica et Cosmochimica Acta*, 57, 4769–4783.
- Hughes, J.M., Jolliff, B.L., and Gunter, M.E. (2006) The atomic arrangement of merrillite from the Fra Mauro Formation, Apollo 14 lunar mission: The first structure of merrillite from the Moon. *American Mineralogist*, this volume.
- James, O.B., Lindstrom, M.M., and Flohr, M.K. (1987) Petrology and geochemistry of alkali gabbroites from lunar breccia 67975. Proceedings of the 17th Lunar and Planetary Science Conference, in *Journal of Geophysical Research*, 89, E314–E330.
- Jarosewich, E. and Boatner, L.A. (1991) Rare-earth reference samples for electron microprobe analysis. *Geostandards Newsletter*, 15, 397–399.
- Jolliff, B.L. (1991) Fragments of quartz monzodiorite and felsite in Apollo 14 soil particles. *Lunar and Planetary Science*, 21, 101–118.
- — — (1993) A monazite-bearing clast in Apollo 17 melt breccia. *Lunar and Planetary Science*, XXIV, 725–726 (abstract).
- Jolliff, B.L., Haskin, L.A., Colson, R.O., and Wadhwa, M. (1993) Partitioning in REE-saturating minerals: Theory, experiment, and modelling of whitlockite, apatite, and evolution of lunar residual magmas. *Geochimica et Cosmochimica Acta*, 57, 4069–4094.
- Jolliff, B.L., Freeman, J.J., and Wopenka, B. (1996) Structural comparison of lunar, terrestrial, and synthetic whitlockite using laser Raman microprobe spectroscopy. *Lunar and Planetary Science*, XXVII, 613–614 (abstract).
- Jolliff, B.L., Floss, C., McCallum, I.S., and Schwartz, J.M. (1999) Geochemistry, petrology, and cooling history of 14161,7373: A plutonic lunar sample with textural evidence of granitic-fraction separation by silicate-liquid immiscibility. *American Mineralogist*, 84, 821–837.
- Keil, K., Prinz, M., and Bunch, T.E. (1971) Mineralogy, Petrology, and chemistry of some Apollo 12 samples. Proceedings of the Second Lunar Science Conference, 2, 319–341.
- Korotev, R.L., Rockow, K.M., Jolliff, B.L., and Haskin, L.A. (1997) Lithic fragments of the Cayley Plains. *Lunar and Planetary Science*, XXVIII, 753–754 (abstract).
- Kostiner, E. and Rea, J.R. (1976) The crystal structure of manganese-whitlockite, $\text{Ca}_{18}\text{Mn}_2\text{H}_2(\text{PO}_4)_{14}$. *Acta Crystallographica*, B32, 250–253.
- Lindstrom, M.M., Crozaz, G., and Zinner, E. (1985) REE in phosphates from lunar highlands cumulates: An ion probe study. *Lunar and Planetary Science*, XVI, 493–494 (abstract).
- Lovering, J.F., Wark, D.A., Gleadow, A.J.W., and Britten, R. (1974) Lunar monazite: A late-stage (mesostasis) phase in mare basalts. *Earth and Planetary Science Letters*, 21, 164–168.
- Lundberg, L.L., Crozaz, G., McKay, G., and Zinner, E. (1988) Rare earth element carriers in the Shergotty meteorite and implications for its chronology. *Geochimica et Cosmochimica Acta*, 52, 2147–2163.
- McKay, G., Wagstaff, J., Le, L., Lindstrom, D., and Colson, R. (1987) Whitlockite/melt partitioning and Henry's Law: Shergotty late-stage minerals. *Lunar and Planetary Science*, XVIII, 625–626 (abstract).
- McSween, H.Y., Jr. (1994) What we have learned about Mars from SNC meteorites. *Meteoritics*, 29, 757–779.
- McSween, H.Y., Jr. and Treiman, A.H. (1998) Martian meteorites (Ch. 6). In J.J. Papike, Ed., *Planetary Materials*, 36, p. 6-01–6-40. Reviews in Mineralogy, Mineralogical Society of America, Chantilly, Virginia.
- Meyer, C. (1996) *Mars Meteorite Compendium—1996*. JSC Publication no. 27672, 175 p. Lyndon B. Johnson Space Center, Houston, Texas.
- Neal, C.R., Taylor, L.A., and Patchen, A.D. (1990) The dichotomy between primitive highland cumulates and evolved interstitial whitlockites: The process of “REEP-fraction” metasomatism. *Lunar and Planetary Science*, XXI, 863–864 (abstract).
- Prewitt, C.T. and Rothbard, D.R. (1975) Crystal structures of meteoritic and lunar whitlockites. *Lunar and Planetary Science*, VI, 646–648 (abstract).
- Quick, J.E., James, O.B., and Albee, A.L. (1981) Petrology and petrogenesis of lunar breccia 12013. Proceedings of the 12th Lunar and Planetary Science Conference (12B), p. 117–172.
- Reed, S.J.B. and Smith, D.G.W. (1985) Ion probe determination of rare earth elements in merrillite and apatite in chondrites. *Earth and Planetary Science Letters*, 72, 238–244.
- Rubin, A.E. (1997) Mineralogy of meteorite groups. *Meteoritics and Planetary Science*, 32, 231–247.
- Shervais, J.W., Taylor, L.A., Laul, J.C., and Smith, M.R. (1985) Correction to “Pristine highland clasts in consortium breccia 14305: Petrology and geochemistry.” Proceedings of the 15th Lunar and Planetary Science Conference, in *Journal of Geophysical Research*, 90, C844.
- Smith, J.V. and Steele, I.M. (1976) Lunar mineralogy, a heavenly detective story. *American Mineralogist*, 61, 1059–1116.
- Wadhwa, M., Crozaz, G., and McSween, H.Y., Jr. (1994) Petrogenesis of shergottite meteorites inferred from minor and trace element microdistributions. *Geochimica et Cosmochimica Acta*, 58, 4213–4229.
- Wang, A., Kuebler, K.E., Jolliff, B.L., and Haskin, L.A. (2004) Raman spectroscopy of Fe-Ti-Cr-oxides, case study: martian meteorite EETA79001. *American Mineralogist*, 89, 665–680.
- Zeigler, R.A., Korotev, R.L., Jolliff, B.L., and Haskin, L.A. (2005) Petrology and geochemistry of the LaPaz Icefield basaltic lunar meteorite and source-crater pairing with Northwest Africa 032. *Meteoritics and Planetary Science*, 40, 1073–1102.
- Zinner, E. and Crozaz, G. (1986) A method for the quantitative measurement of rare earth elements in the ion microprobe. *International Journal of Mass Spectrometry and Ion Processes*, 69, 17–38.

MANUSCRIPT RECEIVED DECEMBER 12, 2005

MANUSCRIPT ACCEPTED JUNE 4, 2006

MANUSCRIPT HANDLED BY C. SHEARER